doi:10.1093/brain/awx009 BRAIN 2017: 140; 981–997 | 981

BRAIN
A JOURNAL OF NEUROLOGY

Photosensitive epilepsy is associated with reduced inhibition of alpha rhythm generating networks

Anna Elisabetta Vaudano,[1,2,*] Andrea Ruggieri,[1,2,*] Pietro Avanzini,[3] Giuliana Gessaroli,[2] Gaetano Cantalupo,[4] Antonietta Coppola,[5] Sanjay M. Sisodiya[6,7] and Stefano Meletti[1,2]

[*]These authors contributed equally to this work.

See Hamandi (doi:10.1093/awx049) for a scientific commentary on this article.

Photosensitivity is a condition in which lights induce epileptiform activities. This abnormal electroencephalographic response has been associated with hyperexcitability of the visuo-motor system. Here, we evaluate if intrinsic dysfunction of this network is present in brain activity at rest, independently of any stimulus and of any paroxysmal electroencephalographic activity. To address this issue, we investigated the haemodynamic correlates of the spontaneous alpha rhythm, which is considered the hallmark of the brain resting state, in photosensitive patients and in people without photosensitivity. Second, we evaluated the whole-brain functional connectivity of the visual thalamic nuclei in the various populations of subjects under investigation. Forty-four patients with epilepsy and 16 healthy control subjects underwent an electroencephalography-correlated functional magnetic resonance imaging study, during an eyes-closed condition. The following patient groups were included: (i) genetic generalized epilepsy with photosensitivity, 16 subjects (mean age 25 ± 10 years); (ii) genetic generalized epilepsy without photosensitivity, 13 patients (mean age 25 ± 11 years); (iii) focal epilepsy, 15 patients (mean age 25 ± 9 years). For each subject, the posterior alpha power variations were convolved with the standard haemodynamic response function and used as a regressor. Within- and between-groups second level analyses were performed. Whole brain functional connectivity was evaluated for two thalamic regions of interest, based on the haemodynamic findings, which included the posterior thalamus (pulvinar) and the medio-dorsal thalamic nuclei. Genetic generalized epilepsy with photosensitivity demonstrated significantly greater mean alpha-power with respect to controls and other epilepsy groups. In photosensitive epilepsy, alpha-related blood oxygen level-dependent signal changes demonstrated lower decreases relative to all other groups in the occipital, sensory-motor, anterior cingulate and supplementary motor cortices. Coherently, the same brain regions demonstrated abnormal connectivity with the visual thalamus only in epilepsy patients with photosensitivity. As predicted, our findings indicate that the cortical-subcortical network generating the alpha oscillation at rest is different in people with epilepsy and visual sensitivity. This difference consists of a decreased alpha-related inhibition of the visual cortex and sensory-motor networks at rest. These findings represent the substrate of the clinical manifestations (i.e. myoclonus) of the photoparoxysmal response. Moreover, our results provide the first evidence of the existence of a functional link between the circuits that trigger the visual sensitivity phenomenon and those that generate the posterior alpha rhythm.

1 Department of Biomedical, Metabolic, and Neural Science, Center for Neuroscience and Neurotechnology, University of Modena and Reggio Emilia, OCSE Hospital, Modena, Italy
2 Neurology Unit, OCSAE Hospital, Azienda Ospedaliera Universitaria, Modena, Italy
3 Department of Neuroscience, University of Parma, Consiglio nazionale delle Ricerche — CNR, Parma, Italy
4 Department of Life and Reproduction Sciences, University of Verona, Verona, Italy
5 Epilepsy Centre, Department of Neuroscience, Odontostomatology and Reproductive Sciences, Federico II University, Naples, Italy
6 Department of Clinical and Experimental Epilepsy, UCL Institute of Neurology, National Hospital for Neurology and Neurosurgery, LondonWC1N 3BG, UK

Received June 15, 2016. Revised November 10, 2016. Accepted December 11, 2016. Advance Access publication February 20, 2017

7 Epilepsy Society, Chalfont-St-Peter, Bucks SL9 0RJ, UK

Correspondence to: Stefano Meletti,
Department of Biomedical,
Metabolic, and Neural Science,
University of Modena and Reggio Emilia,
NOCSE Hospital,
via Giardini 1355, 41126 Modena,
Italy
E-mail: stefano.meletti@unimore.it

Keywords: photosensitivity; epilepsy; alpha rhythm; BOLD; functional connectivity

Abbreviations: BOLD = blood oxygen level-dependent; EEG-fMRI = simultaneous recording EEG and functional MRI; EMA = eyelid myoclonia with absences; GGE = genetic generalized epilepsy; ICA = independent component analysis

Introduction

Photosensitivity refers to a condition in which epileptiform activity is induced by flickering lights, such as flashing lights on television or as produced by video games on computer screens. As an EEG trait, it is characterized by the occurrence of a photoparoxysmal response during intermittent photic stimulation (Kasteleijn-Nolst Trenitè *et al.*, 2001) and it is reported in about 10% of patients with epilepsy compared with $<0.5\%$ in otherwise healthy individuals (Gregory *et al.*, 1993). Photosensitivity is the distinctive hallmark of photosensitive occipital lobe epilepsy, which is a focal reflex epilepsy syndrome (Guerrini *et al.*, 1995), and Jeavons syndrome (Jeavons, 1977), which is characterized by eyelid myoclonia, with or without impaired consciousness, on eye closure. Visual sensitivity is also frequently reported as a reflex trait in patients with genetic generalized epilepsies (GGE, formerly known as idiopathic generalized epilepsies), particularly juvenile myoclonic epilepsy, for which the incidence of photosensitivity ranges from 30% (Wolf and Goosses, 1986) to 90% (Appleton *et al.*, 2000) of patients. The high heritability of photosensitivity is widely recognized. Recent evidence points to *CHD2* as a novel gene implicated in photosensitive epilepsy, with patients exhibiting a higher prevalence of unique *CHD2* variants than a control cohort representative of the general population (Galizia *et al.*, 2015).

Precipitation of seizures in photosensitive patients inevitably depends on the activation of a critical neuronal population in the occipital cortex (Wilkins *et al.*, 2004). The distinguishing feature of photosensitive individuals seems to lie in intrinsic hyperexcitability of the visual cortex, which can predispose to large-scale neuronal synchronization. Studies of visual evoked potentials and transcranial magnetic stimulation in patients with photosensitive GGE (Strigaro *et al.*, 2012, 2015; Brigo *et al.*, 2013) identified an abnormal excitability profile of the visual cortex, which co-existed with defective contrast gain control mechanisms (Porciatti *et al.*, 2000). However, although hyperexcitability of the visual cortex explains some ictal and EEG findings, it does not entirely elucidate the range of photosensitivity–associated EEG and clinical correlates. Indeed, photoparoxysmal responses are often generalized, and photic stimulation ultimately can elicit seizures with motor components, which are a particularly frequent reflex trait in patients with GGE.

Previous EEG-correlated functional MRI (EEG-fMRI) studies have detected photoparoxysmal-related activation in parietal and premotor cortices (Moeller *et al.*, 2009; Bartolini *et al.*, 2014). We recently elucidated the blood oxygen level-dependent (BOLD) response to eye-closure in patients with Jeavons Syndrome, discovering the involvement of substantially the same brain circuits (Vaudano *et al.*, 2014). Interestingly, both the study of Vaudano *et al.* (2014), and the study of Moeller *et al.* (2009), reveals the presence of an abnormal increase of BOLD signal before the appearance of spike and wave discharges, thus underscoring the possibility that signal changes might be linked to intrinsic dysfunction of this network.

Taken together, current data indicate that photosensitivity is the expression of an alteration of the visual system, not only limited to the occipital cortex, but expressed as an extended and functional system. For this reason, we believe that a fundamental question, still substantially not investigated, concerns the neural correlates of the alpha rhythm in photosensitive patients. The alpha rhythm, first described by Berger (1929), represents the posterior rhythm of the brain. Historically, alpha oscillations have been considered an idling rhythm, indicating inactivity of brain regions (Pfurtscheller *et al.*, 1996). More recently, this view has changed, towards a functional role of alpha oscillation in inhibiting neural regions not relevant to the task-related context (Klimesch *et al.*, 2007; Mazaheri and Jensen, 2010). Therefore, alpha oscillations in the primary visual areas may represent a mechanism to modulate incoming information. This 'gating function' theory, along with the classical alpha desynchronization, predicts greater alpha activity (i.e. greater alpha power) in inhibited cortical areas and lower alpha activity (i.e. lower alpha power) in areas engaged in information processing (Volkmann, 1986; Toscani *et al.*, 2010).

Recently, concurrently recorded EEG-fMRI has been used to search the entire brain for metabolic and/or haemodynamic correlates of the posterior alpha rhythm (Goldman *et al.*, 2002; Laufs *et al.*, 2003, 2006; Moosmann *et al.*,

2003; Feige *et al.*, 2005; de Munck *et al.*, 2007; Tyvaert *et al.*, 2008; Sadaghiani *et al.*, 2010). The cortical correlation between the posterior alpha modulation and the BOLD signal was negative in every study: the higher the power of the alpha rhythm, the lower was the BOLD signal. The inverse alpha–BOLD signal correlation is evident and maximal over the posterior visual areas, but extends to parietal and prefrontal cortical regions in the majority of studies.

Based on this knowledge, we tested the hypothesis that the haemodynamic correlates of the alpha rhythm in photosensitive patients are different with respect to normal subjects and people with epilepsy without photosensitivity. We used EEG-fMRI to find out if the fluctuations in the alpha rhythm correlate with changes in the BOLD signal in cortical and subcortical regions. Specifically, we predicted that alpha-related BOLD signal decreases in the visual system (and beyond, as demonstrated in previous studies) are reduced in photosensitive patients. Then, we evaluated the whole-brain functional connectivity of the visual thalamus (pulvinar), a region implicated in the genesis of the alpha rhythm in animals and humans (Moruzzi and Magoun, 1949; Lopes da Silva *et al.*, 1973, 1980; Chatila *et al.*, 1993; Hughes and Crunelli, 2005; Liu *et al.*, 2012).

Materials and methods

Study populations and settings

We retrospectively reviewed the entire cohort of patients with epilepsy who underwent an EEG-fMRI study for different purposes, between September 2008 and September 2015, in our Department (total of 260 patients). For the purpose of this study, only patients who had a good quality, 10 min resting state functional MRI recording with eyes-closed and that fulfilled the following inclusion criteria, were considered: (i) older than 16 years of age; (ii) normal structural brain MRI on conventional diagnostic protocol at 3 Tesla; and (iii) absence of sleep EEG figures and absence of interictal events during scanning, or with fewer than 2 spikes/min. Patients with epileptic encephalopathy were excluded from this study.

We therefore focused on a pool of 44 patients affected by the following epileptic syndromes (according to the definitions of the Commission on Classification and Terminology of the International League Against Epilepsy) (Berg *et al.*, 2010).

Genetic generalized epilepsies with photosensitivity

This group of patients (GGE PS+) consisted of 16 subjects (mean age 25 ± 10 years), 11 female and five males. For all these patients, a 32-channel EEG recording was available within the 3 months before the functional MRI study with an intermittent photic stimulation protocol according to international guidelines (Kasteleijn-Nolst Trenite *et al.*, 1999). Photosensitivity was diagnosed if subjects had a photoparoxysmal response to intermittent photic stimulation (Kasteleijn-Nolst Trenité *et al.*, 2001). In all patients, the photoparoxysmal response consisted of generalized spike and wave discharges (type III and IV photoparoxysmal response, Waltz *et al.*, 1992).

Patients had either juvenile myoclonic epilepsy or Jeavons syndrome (eyelid myoclonia with absences, EMA) (Jeavons, 1977). The specific inclusion criteria for diagnosis of EMA, beyond the presence of photosensitivity, were the following: (i) age of onset between 2 and 14 years; (ii) eyelid myoclonus with or without absences; (iii) related generalized paroxysmal activity; and (iv) eye-closure-induced seizures, EEG paroxysms or both (within 0.5–4 s after eye-closure) (Appleton *et al.*, 1993; Giannakodimos and Panayiotopoulus, 1996; Striano *et al.*, 2002). At the time of the study, self-induction was not reported by any patient. All patients had a photoparoxysmal response with eyelid flickering.

Genetic generalized epilepsies without photosensitivity

This group of patients consisted of 13 subjects (mean age 25 ± 11 years), nine female and four males. Patients had syndromic diagnoses of juvenile absence epilepsy or GGE with tonic-clonic seizures only and are termed GGE PS−.

Focal non-lesional epilepsy group

This group of patients consisted of 15 subjects (mean age 25 ± 9 years), 10 female and five males. These patients were affected by cryptogenic focal epilepsy (normal structural MRI). All had clear focal interictal discharges and seizures with or without impairment of consciousness.

None of the patients belonging either to GGE PS− and focal epilepsy groups ever showed photoparoxysmal response to photic stimulation or abnormal sensitivity on eye-closure in previous EEG recordings.

Table 1 reports the demographic and electroclinical variables of the three epilepsy groups. Per protocol, all patients were administered a general intelligence evaluation within 1 to 6 months prior to functional MRI recordings [Wechsler Adult Intelligence Scale – Fourth Edition (WAIS-IV)]. Full-scale IQ was within the normal range in all recruited subjects.

Sixteen healthy volunteers (controls) (10 female and six male subjects, mean age 25 ± 5 years), with no history of neurologic or psychiatric disorders, participated in the study.

The four study groups (the three epilepsy groups and the control group) had the same age and gender distribution. Neither patients nor controls had been taking neuroactive drugs (alcohol and caffeine included) for 72 h prior to the study, except for the patients' antiepileptic treatment. Valproic acid (VPA) is a drug that in previous studies has been demonstrated to lower brain rhythm power (Larsson *et al.*, 2005, 2012; Clemens *et al.*, 2007). VPA was taken by 9/16 GGE PS+ patients, by 8/13 GGE PS− patients and by 4/15 focal epilepsy patients. The mean VPA dose in each group was 750 ± 200 mg/day (GGE PS+), 800 ± 300 mg/day (GGE PS−), and 800 ± 200 mg/day (focal epilepsy), with no significant difference between groups (one-way ANOVA, $P > 0.1$).

Subjects' neurological and ophthalmologic examinations were normal. All subjects were right-handed based on the Edinburgh Handedness Inventory.

The human ethics committee of the University of Modena and Reggio Emilia approved this study. Written informed consent was obtained from all subjects or their parents if underage.

Table 1 Demographic and electroclinical variables of selected patients

			Electroclinical details			IEDs during functional MRI	
Patient ID	**Age**	**Sex**	**ILAE syndrome**	**IEDs type**	**AEDs**	**IEDs, *n***	**Mean length (s)**
GGE PS+							
1	17	M	EMA	GSW	VPA	0	0
2	29	F	EMA	GSW	LEV; VPA	1	3.43
3	56	F	EMA	GSW	VPA	0	0
4	35	F	EMA	GSW	LTG; CLB	0	0
5	30	F	EMA	GSW	VPA	0	0
6	26	F	EMA	GSW	LEV; VPA	2	3.72
7	20	F	EMA	GSW	VPA, LTG	0	0
8	21	F	EMA	GSW	LEV	0	0
9	20	M	EMA	GSW	VPA	2	3.78
10	17	M	EMA	GSW	PB; ZNS; ETS	0	0
11	17	F	EMA	GSW	LEV	1	2.05
12	20	F	EMA	GSW	ETS; VPA	2	2.23
13	35	F	JME	GSW	VPA	2	1.45
14	19	F	JME	GSW	LEV	0	0
15	28	M	JME	GSW	PB; TPM	0	0
16	18	M	JME	GSW	LEV	2	2.57
GGE PS–							
1	33	F	JAE	GSW	–	2	3.17
2	17	F	JAE	GSW	LEV	0	0
3	53	M	JAE	GSW	LEV; VPA	0	0
4	20	M	JAE	GSW	VPA	3	0.91
5	21	F	JAE	GSW	VPA	0	0
6	24	F	JAE	GSW	LEV; CLB	0	0
7	18	F	JAE	GSW	VPA	0	0
8	17	M	JAE	GSW	VPA	0	0
9	18	F	JAE	GSW	VPA	0	0
10	28	M	JAE	GSW	VPA; LEV	1	3.99
11	41	F	GGE with TC	GSW	PB	1	1.46
12	16	F	JAE	GSW	LEV	0	0
13	24	F	GGE with TC	GSW	VPA; TPM	0	0
Focal epilepsy							
1	19	F	FE	R Fr-T S	LEV; OXC	0	0
2	30	F	FE	R P SW	CBZ	0	0
3	30	F	FE	L T S	LTG; CBZ; LEV	0	0
4	50	F	FE	L T SW	OXC; LEV	7	<1
5	23	F	FE	R T S	LCM; VPA	0	0
6	33	F	FE	R Fr-T SW	CBZ; VPA	0	0
7	17	F	FE	L C-T SW	–	5	<1
8	16	F	FE	L Fr-T ShW	LEV; PB; CBZ	0	0
9	23	M	FE	R Fr SW	VPA	6	<1
10	18	M	FE	R T SW	CBZ; VPA	0	0
11	19	F	FE	L Fr-T S	OXC	0	0
12	19	M	FE	B C-T S	–	L 4; R 5	<1
13	32	M	FE	LT S	LEV; TGB; LCM	0	0
14	35	F	FE	R T SW	OXC	0	0
15	22	M	FE	L T SW	OXC; LEV	0	0

AEDs = antiepileptic drugs; B = bilateral; C = central; CBZ = carbamazepine; CLB = clobazam; ETS = etosuccimide; F = female; Fr = frontal; FE = focal epilepsy; GGE with TC = genetic generalized epilepsies with tonic-clonic seizures only; GSW = generalized spike and wave; IEDs = interictal epileptic discharges; JAE = juvenile absence epilepsy; JME = juvenile myoclonic epilepsy; L = left; LCM = lacosamide; LEV = levetiracetam; LTG = lamotrigine; M = male; O = occipital; OXC = oxcarbamazepine; P = parietal; PB = phenobarbital; R = right; S = spike; ShW = sharp wave; SW = spike and wave; T = temporal; TGB = tiagabine; TPM = topiramate; VPA = valproate; ZNS = zonisamide.

EEG recordings

Scalp EEG was recorded by means of a 32-channel MRI-compatible EEG recording system (Micromed). Electrodes were placed according to conventional 10–20 locations. FCz was the reference. ECG was recorded from two chest electrodes. Electrode impedance was kept below 10 kΩ. Prior to in-magnet EEG recording, 10 min of out-of-magnet EEG data were collected in a room adjacent to the scanner. Foam pads were used to help secure the EEG leads, minimize motion, and improve patient comfort. Data were transmitted via a fibre optic cable from the high-input impedance amplifier (5 kHz sampling rate) to a computer located outside the scanner room. To avoid saturation, the EEG amplifier had a resolution of 22 bits with a range of ± 25.6 mV. An anti-aliasing hardware band-pass filter was applied with a bandwidth between 0.15–269.5 Hz.

Subjects' behaviour was constantly observed and recorded by means of a small camcorder positioned on the head coil inside the scanner pointing to the patient's face to obtain split-screen video-EEG documentation during the functional MRI recording (Ruggieri *et al.*, 2015).

The subjects were asked to rest with eyes closed, to not sleep, and to keep still during functional MRI acquisitions. All recordings were performed in the early afternoon in a dimly-illuminated room with a constant luminance (~25 lx). Sedation was never used.

Functional MRI acquisition

Functional data were acquired using a Philips Intera system at 3 T and a gradient-echo echo-planar sequence from 30 axial contiguous slices (repetition time = 3000 ms; in-plane matrix = 64 × 64; voxel size: 4 × 4 × 4 mm) over one 10-min session per patient (200 images). A high-resolution T_1-weighted anatomical image was acquired for each patient to allow anatomical localization. The volume consisted of 170 sagittal slices (repetition time = 9.9 ms; echo time = 4.6 ms; in plane matrix = 256 × 256; voxel size = 1 × 1 × 1 mm).

EEG artefact correction and processing

The correction of the gradient artefact was performed offline by means of the Brain Quick System Plus software (Micromed, Mogliano Veneto, Italy) (Allen *et al.*, 2000). The EEG data were then exported in the .edf format and reviewed and analysed by means of the BrainVision Analyzer 2.0 software (Brain Products, Munich, Germany). After downsampling to 250 Hz, a band-pass filter between 1 and 70 Hz was applied to the continuous recording and channels showing high impedance or electrode displacement artefacts were interpolated through a cubic spline. Pulse-related artefacts were removed offline from the EEG trace recorded during scanning using the EEG processing package of Brain Analyzer (Allen *et al.*, 1998).

The preprocessed EEG data were then submitted to an independent component analysis (ICA) as previously described (Avanzini *et al.*, 2014; Ruggieri *et al.*, 2015).

For each participant, the 30 EEG channels signal was decomposed into 30 components (between F0 to F29). Each component resulting from ICA separation is characterized by a time course, describing the morphology of the component over time, and by a specific topography (i.e. an array containing the weights the specific component has in each channel). In patient populations, two expert epileptologists (A.E.V., A.R.) reviewed both the standard EEG recordings and the relative individual components of the ICA-processed recordings to detect interictal epileptic discharges. The independent components that on visual inspection showed interictal epileptic discharges were marked as epi-IC and discarded from subsequent alpha frequency and power estimations. Moreover, to avoid interaction of interictal events or remaining small motion artefacts with the alpha power variation analysis, we replaced the EEG during these events with a signal obtained by interpolating the EEG before and after the event, as previously applied (Tyvaert *et al.*, 2008). For each subject, no more than 5% of the EEG was subjected to interpolation.

Estimation of the alpha power and validation

Supplementary Fig. 1 illustrates the main steps of individual alpha band calculation. The independent components that on visual inspection showed rhythmic activity in the 8–12 Hz band were marked as alpha-related IC (αIC). For all αIC in each subject, the artefact-free time course was divided into 3-s epochs (equal to repetition time) using a Hanning time window (epochs were overlapped by 50%) and submitted to fast Fourier transform (FFT). The relative power was computed between 7.5 and 12.5 Hz with a frequency resolution equal to 0.1 Hz. The FFT revealed a number of αIC ranging from a minimum of two to a maximum of 20 components for each subject. Then, one posterior alpha component originating from the primary visual cortex was selected based on the following criteria: (i) a peak in the alpha range as revealed by FFT; and (ii) a medial-posterior topography of the mixing weights, which expresses the relative strength at which each component time course is expressed at each electrode. This component is reliably observed when ICA is applied to EEG data (Makeig *et al.*, 2004*a*, *b*). Next, for each subject the mean individual alpha frequency (Hz) and its respective power (μV^2/Hz) were calculated for the selected component. Finally, after the ICA component selections, the spectral power of the alpha component of the given subject was integrated across each epoch and used as an 'alpha' regressor for the same subject's functional MRI time series. The resulted regressor quantifies the alpha-band power of the medial-posterior alpha component within each scan interval. The procedure applied to obtain the alpha-regressor is therefore dependent on the ICA methodology.

To ensure the validity of the EEG data and analysis obtained during the functional image acquisition, the same EEG preprocessing and analysis was performed for the 10 min of resting state acquired prior to the functional MRI protocol in each subject. Next, we compared the mean alpha frequency and the mean alpha power of the EEG outside the scanner with those obtained during the scan time.

Functional MRI analysis

Alpha-BOLD correlation

Matlab 7.1 and SPM8 (Wellcome Department of Imaging Neuroscience, London, UK) software were used for functional MRI data analysis. All functional volumes were slice-time corrected, realigned to the first volume acquired, spatially normalized into standard space and smoothed with an $8 \times 8 \times 8$ mm full-width at half-maximum Gaussian kernel.

For first-level analysis, the alpha power variations were convolved with the standard haemodynamic response function, downsampled to the MRI frequency and used as a regressor in a single general linear model. Movement artefacts identified by analysis of video-EEG recordings (blinking, lip smacking, swallowing, head movements) were considered as confounds in the model (Ruggieri *et al.*, 2015). In addition, 24 realignment parameters [six scan realignments parameters from image preprocessing and a Volterra expansion of these (Friston, *et al.*, 1996)] were included in the model as confounds. A t-contrast was specified, testing for the column 'alpha regressor'.

For second-level group analysis, the statistical images resulting from single-subject contrasts were submitted to a second level (group) random-effect analysis to look for effect on the BOLD signal at the population level. A full factorial design, as implemented in SPM8, was used to test for between groups effects (one-way ANOVA; four groups): GGE PS+; GGE PS−; focal epilepsy; and healthy controls. Subject age and sex were included in the model as covariates.

The statistical inferences for first- and second-level analyses were set to the threshold of $P < 0.05$, corrected for family-wise errors (FWE), in order to show significant BOLD changes at the whole-brain level. If there were no clusters surviving at this level, the threshold was changed to $P < 0.05$ corrected for false discovery rate (FDR). Controlling the FDR with the criterion FDR = 0.05 increases the number of false positives relative to FWE techniques, but also increases the ability to detect meaningful signals (Genovese *et al.*, 2002; Nichols and Hayasaka, 2003; Bennett *et al.*, 2009).

The second-level alpha-related functional MRI data and the groups' comparisons were further analysed by means of non-parametric permutation method for multiple-comparisons correction (AFNI_16.1.01, 3dClustSim function, version-February 2016; http://afni.nimh.nih.gov/pub/dist/doc/program_help/3dClustSim.html) to achieve a family-wise error rate (FWER) at $P = 0.05$ at the cluster level (Cox et al., 2016). The non-parametric analysis was performed to properly control the rate of false positive BOLD changes. Recent evidences, indeed, reported a high risk of an inflated false positive rate in functional MRI group analyses using parametric methods with common functional MRI software tools (i.e. SPM, FSL), even when applying a conservative FWE statistical threshold control (Eklund *et al.*, 2012, 2016). In particular, traditional methods fail to account for spatial autocorrelations, and thereby render cluster thresholds that do not adequately control false-positive inferences. We therefore used the spatial autocorrelation function (*acf*) option when using the AFNI programs 3dFWHMx to estimate intrinsic smoothness in the images and 3dClustSim to estimate the probability of false positive clusters (Cox et al., 2016). This option allows for non-Gaussian models and spatial autocorrelation functions, and calculates moments of differences to a larger radius. Group-level analyses were thresholded at the voxel-level at $P < 0.001$ and cluster size of 210, which provides $P < 0.05$ (corrected).

The resulting statistical maps were warped to the PALS-B12 atlas in Caret for visualization purposes (Caret, http://brainvis.wustl.edu/wiki/index.php/Caret:About) (van Essen, 2005).

Resting state functional connectivity

Considering previous studies (Liu *et al.*, 2012) and the group-level results of the current study (see below), two thalamic regions of interest were defined for further functional connectivity analysis. The BOLD signal time course was extracted from each region of interest (5-mm sphere) for each subject by means of marsbar software (http://marsbar.sourceforge.net/). The first region of interest consisted of the bilateral posterior clusters showing negative correlation with the posterior alpha (i.e. the pulvinar); the second region of interest was the bilateral medial dorsal region showing significant positive correlation with the posterior alpha modulation (i.e. medial dorsal nuclei). Both regions of interest served separately as the seed from which the functional connectivity to the rest of the brain was evaluated for all the subjects considered together and for each group independently. The nuisance variables consisting of 24 realignment parameters and three compartment signals (modelling the average signal in the grey matter, white matter, CSF) were included in the model. Then, functional connectivity maps of controls and epilepsy subpopulations were evaluated and compared.

Results

Estimation of the alpha power

All the subjects demonstrated a component with a medial posterior topography and a single peak in the alpha frequency range, each within 8–12 Hz, the typical range for this age group as reported in the literature (Nunez *et al.*, 2001) (Fig. 1A). The individual alpha frequency and its respective power were averaged across each subpopulation and compared (ANOVA). Across all the investigated subjects, the individual peak alpha frequency showed a normal distribution within the alpha band, both outside and inside the scanner (Fig. 1B). No group differences were evident when comparing the mean alpha frequency between the different populations (Fig. 1C). On the contrary, the mean alpha power was higher in the GGE PS+ population compared to controls and other epilepsies ($P < 0.01$ for all comparisons) (Fig. 1D). The EEG inside and outside the scanner appeared similar on visual inspection in all the subjects. Nevertheless, the alpha power recorded during functional MRI was reduced in all the investigated populations, with an average power reduction of 30%. The mean power reduction was slightly different across the four investigated cohorts, but there was no significant effect of group on power reduction. This finding is consistent with previous published data (Laufs *et al.*, 2003) and is probably linked to intra-scanner EEG post-processing, especially the gradient artefact suppression algorithm. No difference for

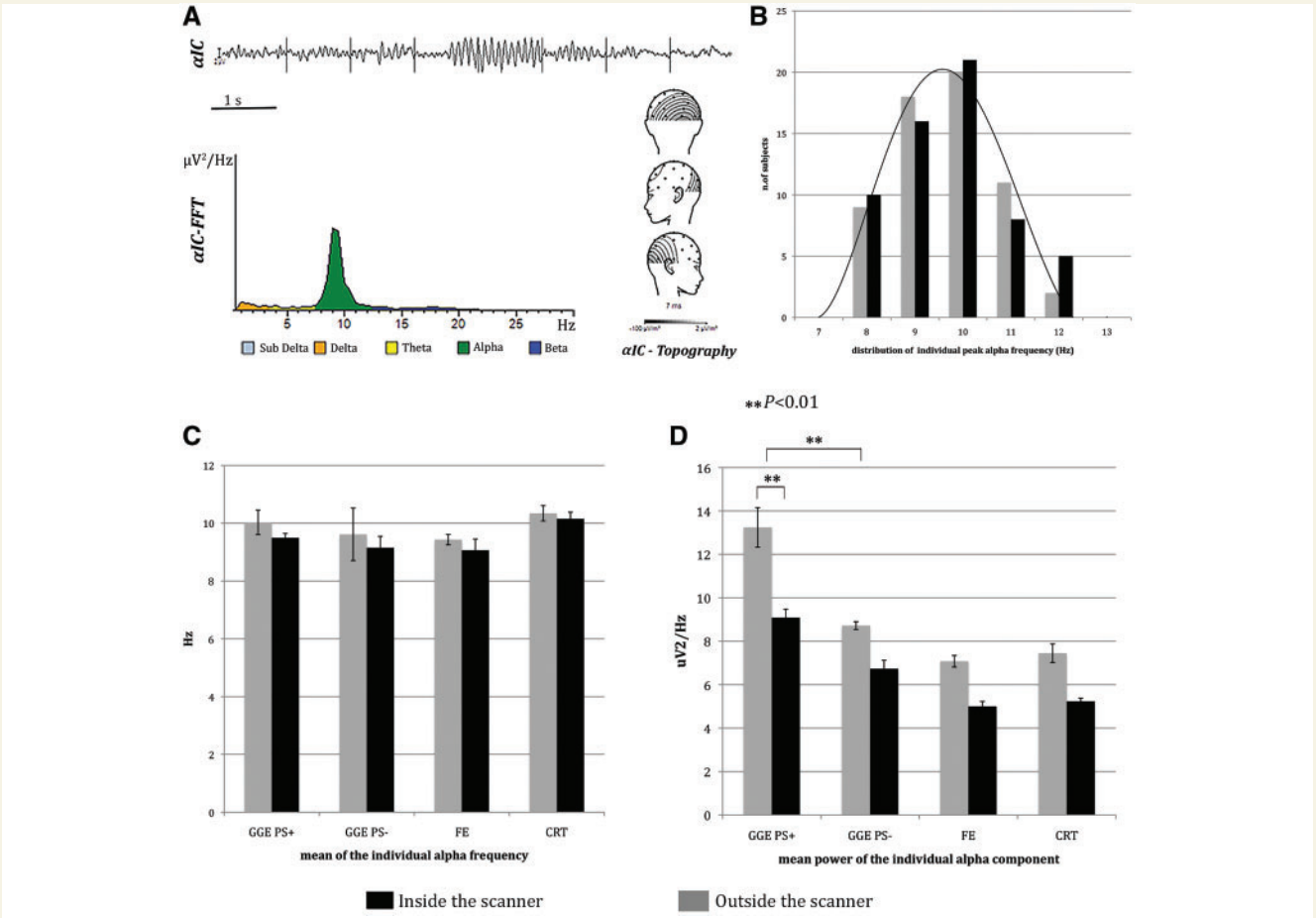

Figure 1 Alpha power estimation and analysis. (**A**) Individual alpha band identification and calculation in a representative example. After visual identification of the αIC (*top*), the posterior alpha component is selected based on the power spectrum (*bottom left*) and average topography (*bottom right*). (**B–D**) Histograms of alpha parameters recorded outside (grey) and inside the scanner (black). (**B**) Histograms show the Gaussian distribution of individual peak alpha frequency within alpha band. (**C**) Histograms illustrate the mean individual alpha frequency in the different subgroups of patients and in controls. (**D**) Histograms display the mean alpha power in the different subgroups of patients and in controls. The GGE PS + shown significantly higher alpha power compared to others both during scanning and outside. The mean alpha power was significantly lower inside then outside the scanner in all the studied population. The bars represent the standard error. $^{**}P < 0.01$. CRT = control; FE = focal epilepsy.

the mean alpha frequency peak was observed comparing the EEG inside, versus outside, the scanner.

Alpha-BOLD correlations: whole population and subgroups results

Second-level whole-population analysis ($n = 60$), as well as subpopulation group findings, did not demonstrate any difference between the applied statistical methods (parametric versus non-parametric). In particular, we did not find cluster mismatches between the two approaches.

When considering all the subjects together the alpha power time series correlated positively with brain activity in the bilateral dorsal cingulate cortex and medial thalamic nuclei and negatively with activity in broad areas of cerebral cortex, including the superior and inferior parietal lobule, the occipital cortex (middle occipital gyrus and lingual gyrus), the precuneus, the premotor and motor regions (supplementary motor area, frontal operculum, precentral cortex), and the middle and superior temporal gyrus. At the subcortical level, the bilateral posterior thalamus, the basal ganglia and brainstem were negatively correlated with the posterior alpha power (Fig. 2A). These findings are concordant with those of previous reports (Goldman *et al.*, 2002; Moosmann *et al.*, 2003; Gonçalves *et al.*, 2006; Difrancesco *et al.*, 2008; Tyvaert *et al.*, 2008; Liu *et al.*, 2012; Omata *et al.*, 2013). Supplementary Table 1 shows the details of the positively and negatively correlated areas. In addition, we used the digital version of the Morel Atlas of the human thalamus (Morel *et al.*, 1997), based on the MNI template (Krauth *et al.*, 2010), to further relate EEG-fMRI findings to specific thalamic nuclei (Fig. 2B). The subcortical thalamic negative correlate of the alpha rhythm was clearly localized at the pulvinar level, and did not involve the lateral geniculate nucleus.

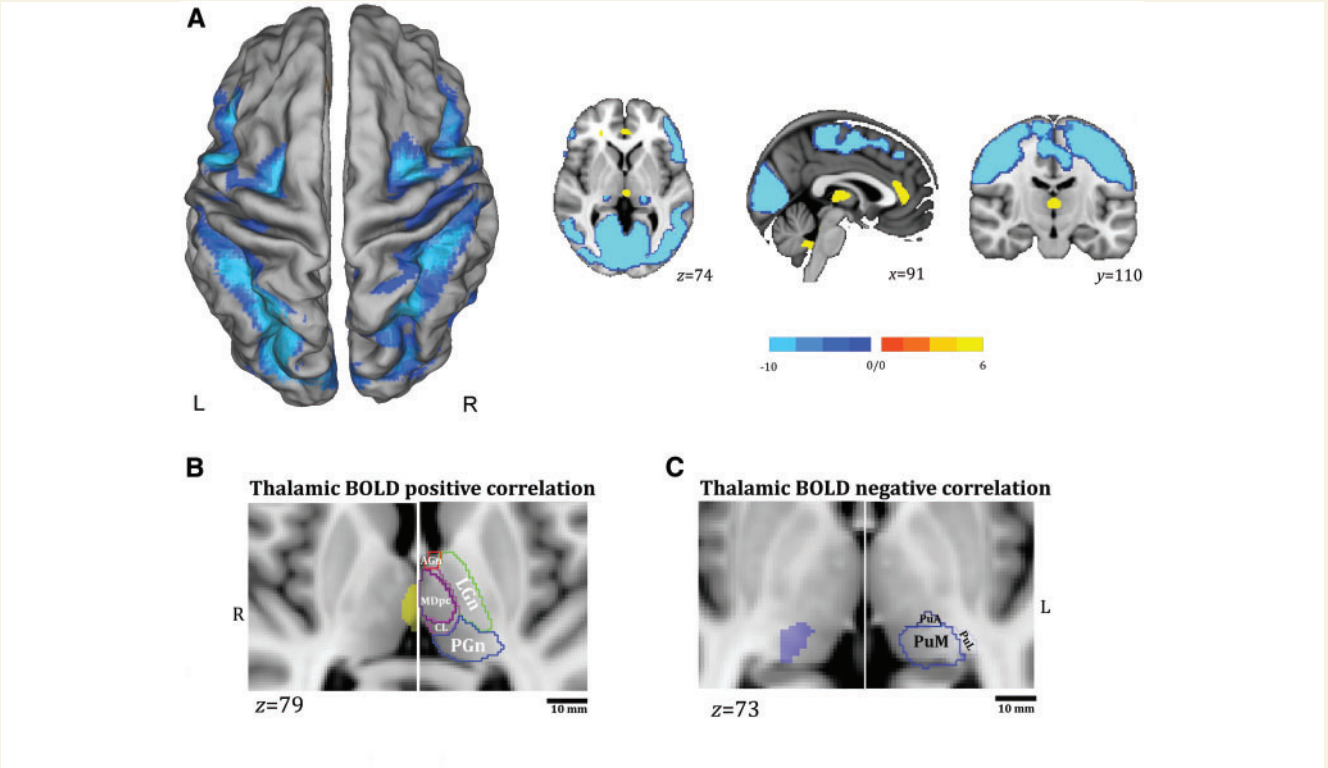

Figure 2 Whole-population BOLD findings. (**A**) Alpha-BOLD correlation map related to all the subjects considered together ($P < 0.05$ corrected for FWE). The functional maps have been warped to the PALS-B12 atlas in caret (dorsal view) for right (R) and left (L) hemisphere (*left*) and overlaid onto representative canonical slices, axial, coronal and sagittal view (*right*) for visualization purposes. The yellow colour identifies the positive correlations to alpha power, the light-blue colour the negative correlations. See text for details. (**B** and **C**) Relationship between BOLD thalamic changes and thalamic nuclei as provided by digital version of the Morel's atlas of human thalamus (Morel *et al.*, 1997; Krauth *et al.*, 2010). Thalamic positive (**B**) ($P < 0.05$ corrected for FDR) and negative (**C**) ($P < 0.05$ corrected for FWE) BOLD correlations are overlaid onto the MNI template (1 mm) (axial slices) as provided by FSL (FMRIB Software Library) after linear transformation using FMRIB Linear Image Registration Tool (FLIRT). For each panel, the localization of the BOLD change is compared with the thalamic atlas. The thalamic atlas is displayed onto the canonical T_1-1 mm image as implemented in FSL (FMRIB Software Library). Canonical T_1 slices are enlarged for visualization purposes. The thalamic nuclei have been indicated by different colours for visualization purposes and grouped according to Morel (1997). LGn, green colour: lateral group of thalamic nuclei that includes the ventroposterior complex, ventral lateral posterior/anterior, and ventral anterior and ventral medial nuclei. AGn, red colour: anterior group of thalamic nuclei that includes anteroventral, anteromedial, anterodorsal, and lateral dorsal nuclei. PGn, blue colour: the posterior group of thalamic nuclei that includes medial and lateral geniculate nuclei, posterior, suprageniculate/limitans, lateral pulvinar nucleus (PuL), medial pulvinar nucleus (PuM) and anterior pulvinar nucleus (PuA). Pink colour shows the mesial group of thalamic nuclei: MDmc = mediodorsal nucleus, magnocellular division; MDpc = mediodorsal nucleus, parvocellular division; CL = Central lateral nucleus. Scale bar = 10 mm. R = right; L = left.

The brain regions that correlated with alpha power in each subpopulation are illustrated in Fig. 3 and summarized in Supplementary Table 2.

The GGE PS+ group showed positive BOLD correlation at the bilateral dorsal cingulate cortex and caudate nucleus. A negative correlation between the alpha predictor and the BOLD signal was found predominantly in the parietal and frontal (motor-premotor) cortical areas. Conversely, the posterior occipital regions [Brodmann area (BA) 18–19] demonstrated a decreased alpha power-related BOLD signal in the other epileptic populations (GGE PS− and focal epilepsy) and in the healthy controls. Parietal, temporal and frontal (motor-premotor) cortical areas were negatively correlated to the alpha in controls, focal epilepsy, and GGE PS− groups with substantial uniformity between them.

Between groups' comparisons

The comparisons of alpha-power BOLD maps between the patient groups and between patients and controls revealed significant differences only for the GGE PS+ population. Specifically, with respect to all other comparisons, GGE PS+ showed a relatively increased BOLD signal in a broad and symmetrical network that includes the pre- and post-central gyrus, the supplementary motor area, the insula, the precuneus and the temporal (BA 20–22) and occipital cortices (BA 18–19) (Fig. 4A). This result is the consequence of a decreased anti-correlation between BOLD signal and alpha power in patients with photosensitivity. No other significant differences were observed either in terms of increased or reduced BOLD correlation to the

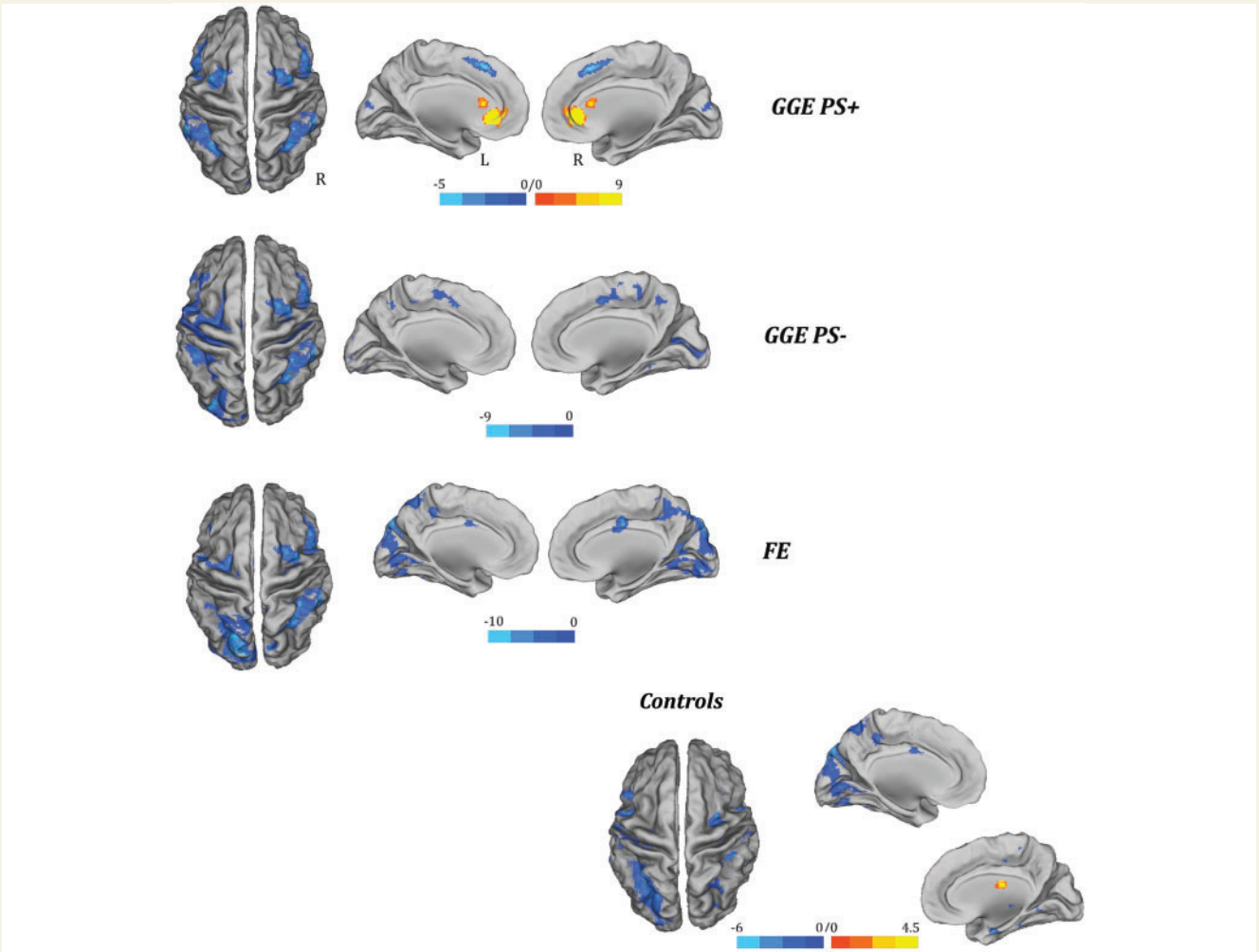

Figure 3 Alpha-BOLD correlation maps related to each single population of subjects ($P < 0.05$, FDR corrected). The functional maps have been warped to the PALS-B12 atlas in caret (mesial and dorsal view) for right (R) and left (L) hemisphere. The yellow-red colour indentifies the positive correlations to alpha power, the light-blue colour the negative correlations. FE = focal epilepsy.

alpha power. Supplementary Table 3 illustrates in detail the results of the between-groups comparisons.

A few differences in terms of total number of clusters identified and relative Z-score were observed applying the non-parametric statistic. However, although a few clusters disappeared, the main BOLD changes survived (Fig. 4B). In particular, the comparison between GGE PS+ and the other cohorts confirmed, in the former, an increased excitability under spontaneous alpha oscillations over the premotor-motor and parieto-occipital cortices (Table 2 and Fig. 4B). Thus, the non-parametric statistical analysis confirms the principal findings of the traditional parametric SPM approach.

Functional connectivity maps

At the population level ($n = 60$), the maps for functional connectivity with the seeds in the medial dorsal nuclei and pulvinar are depicted in Supplementary Fig. 2.

Statistical comparison of the medial dorsal nuclei-related functional connectivity maps between controls and epilepsy subpopulations revealed an increased correlation between resting state BOLD activity in the medial dorsal nuclei and bilateral orbitofrontal cortex (OFC) in GGE PS+ compared to both healthy controls and focal epilepsy patients (Fig. 5). No further differences in functional connectivity maps were detected.

The formal comparison of the pulvinar-related functional connectivity maps between the epilepsy populations, and between patients and controls, revealed again significant differences only for the GGE PS+ subgroup. GGE PS+ demonstrated consistent increased correlation from the pulvinar to the basal ganglia (putamen and caudate), the anterior cingulate cortex, the dorsolateral prefrontal and the parietal cortices with respect to all the other subgroups (GGE PS−, focal epilepsy and controls). Significantly decreased connectivity between the pulvinar and the

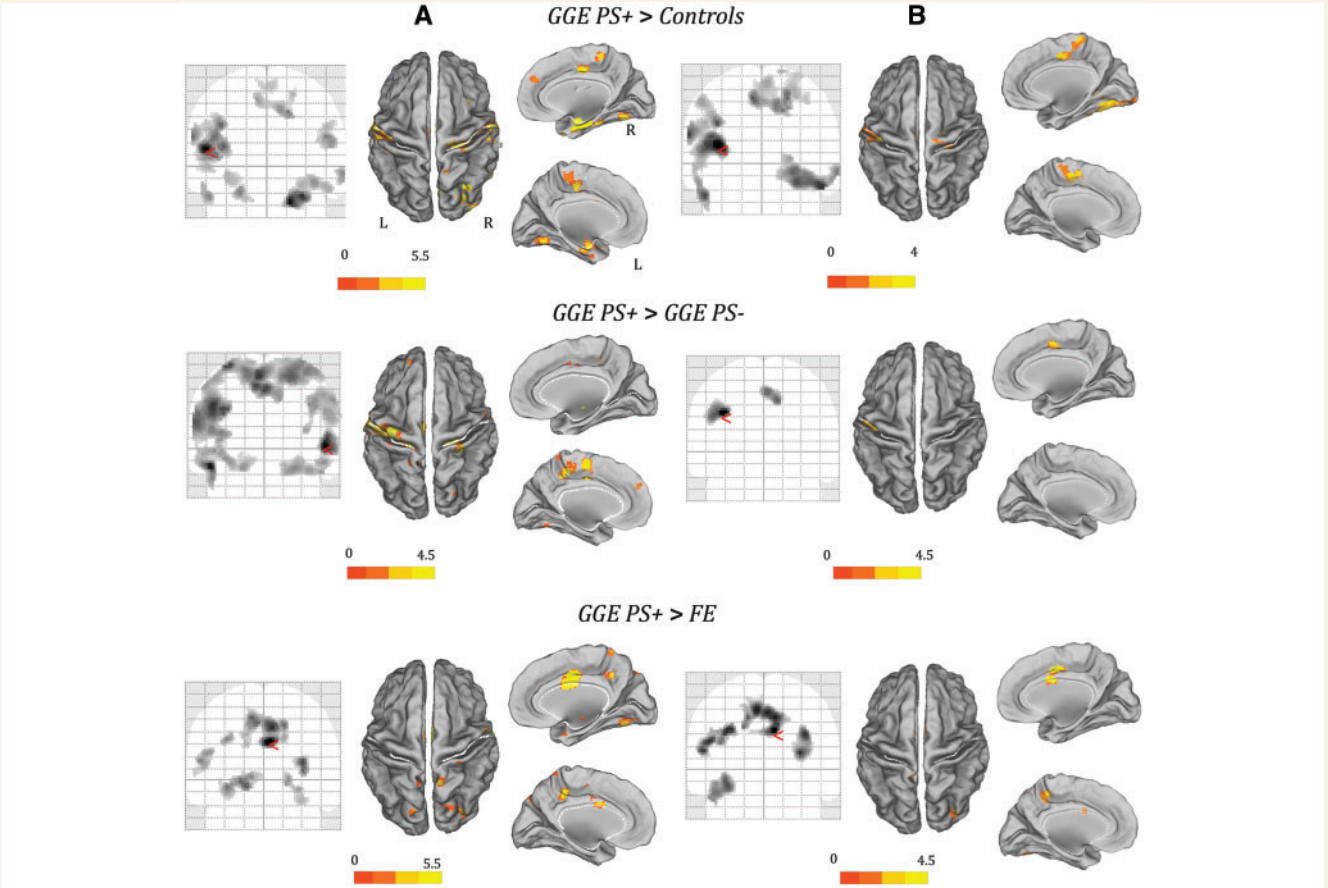

Figure 4 Comparisons of alpha-power BOLD maps between the GGE PS+ group and other patients' cohorts, and between GGE PS+ and control subjects. (**A**) Results of parametric analysis ($P < 0.05$, FDR corrected). (**B**) Results of non-parametric permutation method (AFNI's 3dClustSim function). Only regions survived to statistical threshold of $\alpha < 0.05$ (voxel-wise $P < 0.001$ and cluster size $\geqslant 210$ voxels) are showed. The functional maps are shown on the normalized SPM-glass brain (coronal slices) and warped to the PALS-B12 atlas in caret (mesial and dorsal view) for right (R) and left (L) hemisphere. The red arrow on the SPM-glass brain indicates the global maximum. The white lines on the PALS-B12 atlas show the surface landmarks as implemented in Caret: the central sulcus, the medial wall dorsal segment, and the medial wall ventral segment, the sylvian fissure and calcarine sulcus. FE = focal epilepsy.

somatosensory and visual cortices was observed in the GGE PS+ versus healthy subjects (Fig. 6).

Discussion

This is the first EEG-fMRI investigation of the resting state alpha rhythm in patients with non-lesional focal and GGE, with and without photosensitivity. As predicted, our findings indicate that the cortical-subcortical network generating the alpha oscillation at rest is different in people with epilepsy and visual sensitivity. This difference is independent from the occurrence of overt epileptic activity on scalp EEG and is characterized by: (i) an abnormal haemodynamic coupling between the EEG alpha power fluctuation and the BOLD signal; and (ii) an altered functional connectivity between the pulvinar, which is strongly implicated in generation of the alpha rhythm, and the rest of the brain. Our main finding indicates a reduced alpha-related inhibition in photosensitive epilepsy (i.e. lower BOLD deactivation when alpha power increases) that involves not only the occipital cortex but also extends to the supplementary motor area, the sensorimotor and the premotor cortex. Coherently, the same brain regions demonstrated abnormal connectivity with the visual thalamus only in photosensitive epilepsy.

The alpha rhythm in photosensitive epilepsy

The EEG analysis of the alpha rhythm features showed a significant higher alpha power in GGE PS+ versus other epilepsy groups and controls, confirming a peculiar 'alpha phenotype' of this epileptic trait, at least for the investigated group of photosensitive patients.

Changes of alpha rhythm features have been associated with epilepsy in several neurophysiological studies (Stoller,

Table 2 Alpha-related BOLD maps comparisons obtained using non-parametric permutation method (AFNI's 3dClustSim function)

Brain region	BA	MNI coordinates (mm)			Z-score
		x	y	z	
GGE PS+ > CRT					
L insula	13	−38	−8	14	3.60
B cerebellum	–	48	−58	−20	3.20
L precentral gyrus	4	−64	−6	22	3.08
B middle temporal gyrus	21	−50	0	−28	3.05
B postcentral gyrus	2	−40	−22	32	3.01
L medial frontal gyrus	6	−10	−20	52	2.97
R lingual gyrus	18	24	−76	−8	2.89
GGE PS+ > GGE PS−					
L precentral gyrus	4	−46	−14	30	3.55
R medial frontal gyrus	6	2	−4	50	3.5
GGE PS+ > FE					
B ventral anterior cingulate	24	8	−2	32	4.08
L precentral gyrus	6	−36	−16	32	3.80
L insula	13	−52	−30	22	3.78
B superior occipital gyrus	19	34	−82	28	3.76
L precuneus	7	−16	−56	42	3.54
Middle temporal gyrus	39	−42	−62	22	3.45
B superior temporal gyrus	39	−56	−42	28	3.35

For each subject, the areas showing BOLD signal changes are listed by Z-score value. All reported clusters of activity were corrected for multiple comparisons via Monte Carlo simulations using AFNI's 3dClustSim function (http://afni.nimh.nih.gov/pub/dist/doc/program_help/3dClustSim.html) by ensuring that the size of a given cluster of activation was sufficiently large to rule out discovery by chance (corrected $\alpha < 0.05$ for an uncorrected *P*-value of 0.001 and a 210 voxel cluster size). B = bilateral; R = right; L = left.

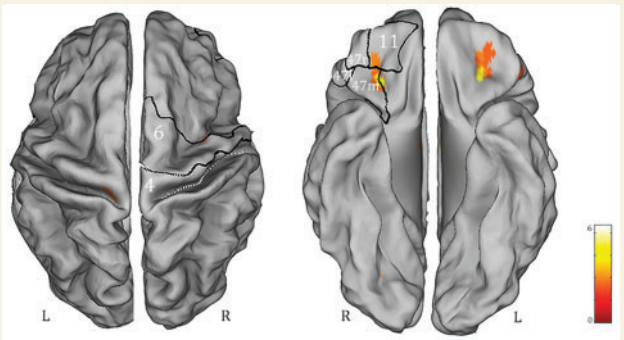

Figure 5 BOLD changes (derived from statistical comparison *P* < 0.05 corrected for FDR) between functional connectivity with seed region at the thalamic medial dorsal nuclei in GGE PS+ versus controls. The resulted map has been warped to the PALS-B12 atlas in caret (dorsal and ventral view) for right (R) and left (L) hemisphere. For localization purposes, functional results on the right hemisphere were plotted and compared against six Brodmann areas indicated by the white numbers. The displayed Brodmann areas cover part of the precentral regions and the orbitofrontal cortex subdivisions (Henssen *et al.*, 2016). Only increases of functional connectivity in GGE PS+ population were detected.

1949; Larsson *et al.*, 2005, 2012; Clemens *et al.*, 2007, 2008; Pyrzowski *et al.*, 2015). The majority of these studies reported a peak alpha frequency reduction in a heterogeneous population of mixed epilepsy phenotypes, rather than changes in alpha power (Miyauchi *et al.*, 1991; Larsson *et al.*, 2005; Clemens *et al.*, 2007; Visani *et al.*, 2010). However, few studies have investigated alpha rhythm features in selected patients with photosensitive epilepsy and compared them with other epilepsy syndromes without photosensitivity (Visani *et al.*, 2010). It should also be underlined that our EEG analysis is based on an ICA of the EEG signal and that the 'alpha regressor' and all alpha calculations were based on the selection of the 'posterior alpha component' on ICA EEG decomposition. This means that the reported alpha features index the oscillatory activity of EEG signal generated from the posterior occipital (calcarine/pericalcarine) cortex. To our knowledge no other study has used this approach to investigate alpha rhythm fluctuation in epilepsy. Considering that this methodology is quite simple and reproducible, and that it could be applied also to routine EEG recordings, it should be relatively straightforward for future studies to test our findings in a larger cohort of photosensitive patients. This also implies that at present it is difficult to directly compare our results with previous studies.

Remarkably, the majority of the patients investigated here were on antiepileptic drug (AED) treatment at the time of the study. In previous studies, changes in the power spectra of intrinsic brain rhythms have been attributed to AED, especially to valproate (Larsson *et al.*, 2005, 2012; Clemens *et al.*, 2007). However, in the current research, an AED effect on alpha power estimation appears unlikely, as valproate and levetiracetam, the AEDs most commonly used in our patients with GGE, were

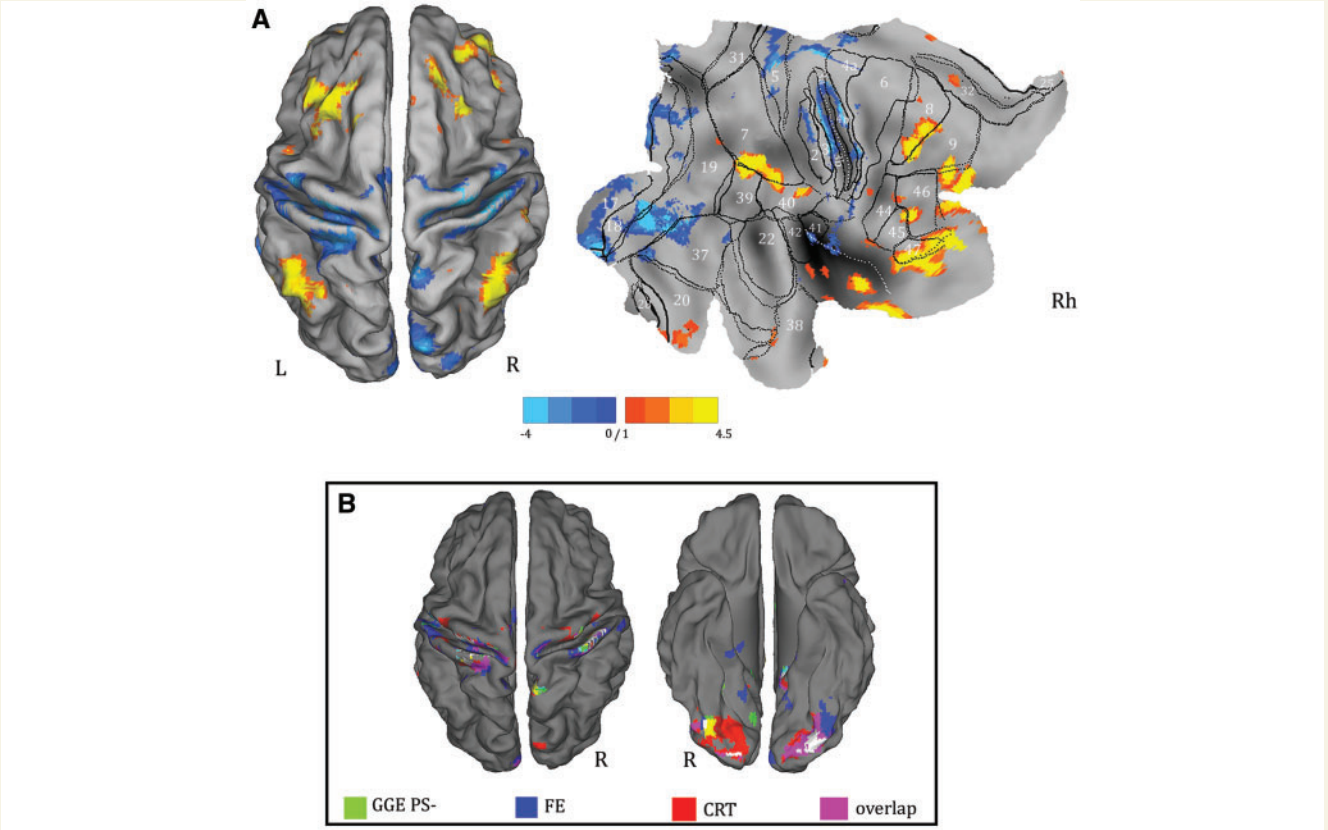

Figure 6 BOLD changes derived from statistical comparison ($P < 0.05$ corrected for FDR) between functional connectivity with seed regions at thalamic pulvinar in GGE PS+ versus control and other epileptic populations. (**A**) Differences in functional connectivity between GGE PS+ and controls. The resulted map has been warped to the PALS-B12 atlas, dorsal view for right (R) and left (L) hemisphere (*left*) and to flat template for the right hemisphere (*right*). For localization purposes, functional results on the right hemisphere (RH) were plotted and compared against Brodmann areas indicated by the white numbers. Increases in functional connectivity are shown in yellow-red, decreases in blue. (**B**) Decreases in functional connectivity in GGE PS+ versus all other population of subjects ($P < 0.05$, uncorrected). Each subjects' subgroup in indicated by a specific colour. The regions coloured in pink represent the overlapping clusters from all the comparisons. CRT = control; FE = focal epilepsy; R = right.

homogenously distributed across PS+ and PS− patients. In particular, the average oral dose of valproate across the different patient groups was similar.

Reduced inhibition in the sensory-motor system in photosensitivity

BOLD correlates of the posterior alpha activity under rest indicated a reduced anti-correlation between the sensory-motor system and the alpha power in patients with photosensitivity (Fig. 4). Classically, BOLD-functional MRI studies reported predominantly negative haemodynamic responses to the alpha oscillations in the occipital lobe (primary and secondary visual cortex) and fronto-parietal cortex (Laufs *et al.*, 2003; Gonçalves *et al.*, 2006; Difrancesco *et al.*, 2008). Overall, negative correlation between the alpha power and the BOLD signal coincides with a decrease of cortical neuronal activity, i.e. a state of inhibition. Indeed, during large-scale synchrony (as in the alpha rhythm), activity in just a small fraction of neurons within a cortical column may be sufficient to give rise to a strong EEG signal, while the inactive majority keeps overall metabolism low and thus the BOLD effect small (Laufs *et al.*, 2003). In this light, the higher haemodynamic signal in the sensory-motor system in GGE PS+ during spontaneous alpha, reflects increased neuronal activity and consequently, we suggest, a lack of inhibition of these regions. This view supports previous observations in photosensitivity by means of neurophysiological and neuroimaging studies, as well as the clinical correlates of photoparoxysmal response that often consist of motor phenomena (i.e. myoclonus, reflecting hyperexcitability). Studies using transcranial magnetic stimulation documented increased visuo-motor hyperexcitability during photic stimulation in GGE patients (Groppa *et al.*, 2008; Strigaro *et al.*, 2012, 2015) and even in healthy individuals with photoparoxysmal response (Siniatchkin *et al.*, 2007). Advanced EEG connectivity analyses show an abnormal pattern, with increased coupling between posterior and anterior frontal areas both at rest and during photoparoxysmal response in patients with

GGE PS+ (Varotto *et al.*, 2012; Moeller *et al.*, 2013). Finally, functional EEG-fMRI studies have detected increased neuronal activity of parietal and premotor cortices during paroxysmal activity evoked by visual stimuli (Moeller *et al.*, 2009; Bartolini *et al.*, 2014).

The brain nodes that demonstrated abnormal behaviour in GGE PS+ under spontaneous alpha oscillations included, beyond the sensory-motor cortex in *strictu sensu*, the premotor regions (supplementary motor area, middle and inferior frontal gyrus) and also non-motor areas in the temporal, parietal and occipital lobes. Notably, the same premotor areas were involved in the abnormal response to eye-closure in patients with EMA (Vaudano *et al.*, 2014), even in the absence of paroxysmal activity on EEG. Overall, our findings confirm and complete the hypothesis of an intrinsic 'visuo-motor hyperexcitability' in GGE PS+. The fact that this upregulation is present under resting (unstimulated) conditions and even during the alpha rhythm, which is considered a hallmark of the brain resting state (Gonçalves *et al.*, 2006), indicates a probable genetic predisposition to generate synchronous paroxysmal activity.

Thalamic contribution to alpha rhythm generation

The correlation between the posterior alpha modulation and the BOLD signal in the thalamus has been reported to be positive (Goldman *et al.*, 2002; Moosmann *et al.*, 2003; Feige *et al.*, 2005; Gonçalves *et al.*, 2006; de Munck *et al.*, 2007; Omata *et al.*, 2013), negative (Lindgren *et al.*, 1999; Moosmann *et al.*, 2003), or even near zero (Laufs *et al.*, 2003). Recently, Liu and colleagues (2012) described both positive and negative correlations between the thalamic nuclei and spontaneous modulation of posterior alpha. Our study is the first that replicates, and thus confirms, the findings that different thalamic nuclei have a different behaviour during alpha rhythm fluctuations. In particular, the negative correlation covers the posterior visual thalamus while positive haemodynamic changes were constrained to the medial dorsal nuclei of the thalamus. The exact contribution of thalamic activity to the cortical oscillations that determine the EEG alpha rhythm is still under investigation. A plausible scheme includes a complex interplay between the primary visual cortex and the visual part (pulvinar and lateral geniculate nucleus) and reticular nuclei of the thalamus (Lopes da Silva *et al.*, 1973, 1980; Fuentealba and Steriande, 2005; Lorincz *et al.*, 2009). Within the posterior thalamic nuclei, the pulvinar, rather than lateral geniculate nucleus, is more likely associated with the spontaneous modulation of posterior alpha rhythm. Animals showing alpha equivalent activity, such as dogs and cats, all have a pulvinar in their visual system, whereas the pulvinar does not seems to exist in brains, such as those of rodents, whose visual system also shows little alpha activity (Hughes and Crunelli, 2005; Pessoa and Adolphs, 2010). In addition the extensive connections of the pulvinar with the entire cortex (Supplementary Fig. 2) (Kaas and Lyon, 2007), make this thalamic nucleus well-suited to behave as the subcortical control hub for widespread cortical alpha activity. Consistently, we also found that the thalamic correlates of alpha power fluctuations involved of the posterior thalamus with preference for the pulvinar over the lateral geniculate nucleus. Furthermore, the cortical regions that were functionally connected to the seed in the pulvinar largely coincided with the cortical regions that were negatively correlated with the posterior alpha rhythm (Fig. 2). As far as the medial dorsal nuclei are concerned, the increased neuronal activity during increased alpha power probably is not directly linked to alpha wave generation, but rather reflects activity related to the arousal level, which is indirectly linked to cortical alpha rhythm fluctuations (Liu *et al.*, 2012; Omata *et al.*, 2013). Indeed, these thalamic nuclei are considered to be part of the ascending reticular activating system, and in particular its dorsal pathways (Moruzzi and Magoun, 1949; Brown *et al.*, 2012).

Thalamo-cortical functional connectivity in photosensitive epilepsy

The whole-brain functional connectivity of the posterior and medial thalamic nuclei was different in photosensitive patients with respect to controls and other epilepsy groups. Notably, it has been recently demonstrated in healthy subjects (Scheeringa *et al.*, 2012) that the increased local alpha synchronization originating from the primary visual cortex is associated with decreased functional MRI resting state connectivity within the visual system. The fact that alpha-band neuronal synchronization is inversely related to connectivity between the primary visual cortex and closely connected regions in both the dorsal and ventral visual stream regions suggests that local alpha-band synchronization in healthy subjects serves to reduce the communication between closely connected regions.

Conversely, GGE PS+ patients had increased resting connectivity of the medial dorsal thalamus-orbitofrontal cortex circuit (Fig. 5). The orbitofrontal cortex (OFC) is a functionally complex structure, which is implicated in high-level cognition processes, and mediates aspects of emotion and behaviour. Other functions have also been linked to OFC activity, including executive control, decision-making, and top-down modulation of bottom-up processes (for review see Damasio, 1995; Elliott *et al.*, 2000). This brain region, and particular the lateral OFC portion (BA11, BA47), has strong connections with the amygdala and insula, structures that are involved in emotional experience and expression (Augustine, 1996; Fink *et al.*, 1996). The fact that this thalamic-prefrontal network is hyper-coupled during rest in patients with photosensitivity might reflect a disruption of cognitive and emotional processes linked to these physiological functions. Notably, juvenile myoclonic epilepsy, in which photosensitivity is commonly observed, has been correlated with psychiatric, behavioural and cognitive

deficits, including those of decision-making and executive control (Wolf *et al.*, 2015). This conclusion remains speculative and further data linking the functional connectivity pattern and neuropsychological and psychiatric profile in GGE PS+ need to be obtained.

When the seed was placed in the pulvinar, GGE PS+ patients demonstrated again a different pattern of cortical resting state connectivity compared to the other populations. Increased connectivity was constrained to the prefrontal cortex (anterior cingulate, dorsolateral prefrontal cortex) and basal ganglia. This visual thalamus-basal ganglia hyper-connectivity could be a promoter of motor cortex hyper-excitability representing a biomarker of increased visuo-motor outflow, which could facilitate myoclonus triggered by visual stimuli. On the contrary, the visual thalamus showed a reduced functional connectivity with the sensory and visual cortex.

The disrupted connectivity between the pulvinar and the visuo-parietal/motor-premotor system further supports the view that photosensitivity in epilepsy is due to abnormal activity of the occipito-frontal circuits, that persists even during rest and independently of visual stimulation and/or pathological paroxysmal activity. Notably, we recently demonstrated by voxel-based morphometry in patients with EMA that the pulvinar also has an abnormal grey matter concentration in these patients, suggesting that microstructural alterations can act over the same pulvinar-fronto-occipital circuit (Vaudano *et al.*, 2014).

Study limitation

We did not explore the haemodynamic correlates of other endogenous EEG frequency bands (i.e. delta, gamma or theta). These additional analyses would be interesting, especially in relation to gamma band activity for the well-known influence of this frequency band in photosensitivity. However, because the data presented here are the first to explore the relationships between spontaneous brain rhythmicity and epilepsy in terms of generating networks, we decide to focus to the alpha rhythm, as a first step.

A possible concern might be related to the decision of applying the ICA methodology to extract the alpha power and obtain the functional MRI regressor. The full-ICA procedure, which decomposes the EEG recording into independent components and the subsequent IC inspection and selection, may sound complex and somehow redundant, as the main target—occipital alpha rhythm—is the most prominent activity on electroencephalographic traces. Previous EEG-fMRI studies on alpha rhythm have used different methods to extract alpha regressors: single or multi-channel averaging, monopolar, bipolar derivations, and ICA (Laufs *et al.*, 2003; Moosmann *et al.*, 2003; Feige *et al.*, 2005; Ritter *et al.*, 2009; Scheeringa *et al.*, 2011, 2012; Mayhew *et al.*, 2013). The overall picture is consistent among the different studies showing an inverse alpha-BOLD relationship involving the posterior cortex as well as parietal and frontal regions. In the present study, the choice of ICA ensures that the EEG-based regressors describe a brain activity as far as possible related to the occipital generators of the alpha rhythm, making them free from volume-conduction and without *a priori* choices that could have weakened or blurred their time course. However, limited to the healthy subjects data, the alpha regressor was also obtained by averaging the signal from parieto-occipital electrodes (P4, O2, P3, O1) without the ICA preprocessing strategy. The alpha-related BOLD signal changes resulted in a similar haemodynamic map to the one detected by means of ICA strategy but with few significant clusters at the threshold of $P < 0.05$ (FDR corrected) (data not shown). Consequently, we applied for all the other analyses the above mentioned ICA strategy to estimate the alpha power fluctuation over time.

Finally, a cautionary note concerns the generalization of the observed alpha rhythm findings. It should be noted that about 70% of the GGE PS+ group comprised subjects affected by Jeavons syndrome (EMA). This means that our EEG (and BOLD) findings could be strongly driven by this subpopulation of photosensitive patients. This is relevant also considering recent genetic findings of a high incidence of *CHD2* mutations in EMA (Galizia *et al.*, 2015). The influence of sub-syndrome effects (i.e. juvenile myoclonic epilepsy versus EMA), as well as the effects of specific genetic defects, will need to be tested in future studies. Finally, although we clearly demonstrated that there is a correlation between alpha rhythm and the BOLD signal (and that this relationship is different in different epilepsy populations), our results do not imply direct causality in either direction.

Conclusion

Our findings provide for the first time, the existence of a functional link between the circuits demonstrated to trigger the photoparoxysmal response and the ones implicated in the generation of the posterior alpha rhythm. As a general conclusion, we suggest that the 'enduring propensity' to generate seizures and/or epileptic activity in patients with photosensitivity is due to the intrinsic susceptibility of a complex thalamo-cortical system, which is indexed by the resting EEG alpha oscillations. One important point of strength of the present work is the use of a multimodal approach to investigate the characteristics of alpha power and the intrinsic networks generating it, resulting in a concordant picture. Our results represent an additional important piece of evidence regarding photosensitivity and contribute to expand the 'system epilepsy' concept (Avanzini *et al.*, 2012) for this epileptic trait.

Acknowledgement

We thank Francesca Benuzzi for helping with EEG-fMRI preparation and acquisition.

Funding

S.M. received research grant support from the Italian Ministry of Health (MOH), from the non-profit organization CarisMO Foundation; A.E. Vaudano received research grant support from the non-profit 'Fondazione Epilessia LICE Onlus' and Italian Ministry of Health (MOH), Emilia-Romagna Region (N. PRUA1GR-2013-00000120). A.R. received a PhD bursary from the University of Modena and Reggio Emilia. The work was partly undertaken at UCLH/UCL, which received a proportion of funding from the Department of Health's NIHR Biomedical Research Centres funding scheme.

Supplementary material

Supplementary material is available at *Brain* online.

References

Allen PJ, Polizzi G, Krakow K, Fish DR, Lemieux L. Identification of EEG events in the MR scanner: the problem of pulse artifact and a method for its subtraction. Neuroimage 1998; 8: 229–39.

Allen PJ, Josephs O, Turner R. A method for removing imaging artifact from continuous EEG recorded during functional MRI. Neuroimage 2000; 12: 230–9.

Appleton RE, Panayiotopoulos CP, Acomb BA, Beirne M. Eyelid myoclonia with typical absences: an epilepsy syndrome. J Neurol Neurosurg Psychiatry 1993; 56: 1312–16.

Appleton R, Beirne M, Acomb B. Photosensitivity in juvenile myoclonic epilepsy. Seizure 2000; 9: 108–11.

Augustine JR. Circuitry and functional aspects of the insular lobe in primates including humans. Brain Res Brain Res Rev 1996; 22: 229–44.

Avanzini P, Vaudano AE, Vignoli A, Ruggieri A, Benuzzi F, Darra F, et al. Low frequency mu-like activity characterizes cortical rhythms in epilepsy due to ring chromosome 20. Clin Neurophysiol 2014; 125: 239–49.

Avanzini G, Manganotti P, Meletti S, Moshé SL, Panzica F, Wolf P, et al. The system epilepsies: a pathophysiological hypothesis. Epilepsia 2012; 53: 771–8.

Bartolini E, Pesaresi I, Fabbri S, Cecchi P, Giorgi FS, Sartucci F, et al. Abnormal response to photic stimulation in juvenile myoclonic epilepsy: an EEG-fMRI study. Epilepsia 2014; 55: 1038–47.

Bennett CM, Wolford GL, Miller MB. The principled control of false positives in neuroimaging. Soc Cogn Affect Neurosci 2009; 4: 417–22.

Berg AT, Berkovic SF, Brodie MJ, Buchhalter J, Cross JH, van Emde Boas W, et al. Revised terminology and concepts for organization of seizures and epilepsies: report of the ILAE Commission on classification and terminology, 2005–2009. Epilepsia 2010; 51: 676–85.

Berger, H. Über das Elektrenkephalogramm des Menschen. Arch Psychiatr Nervenkr 1929; 87: 527–70.

Brigo F, Bongiovanni LG, Nardone R, Trinka E, Tezzon F, Fiaschi A, et al. Visual cortex hyperexcitability in idiopathic generalized epilepsies with photosensitivity: a TMS pilot study. Epilepsy Behav 2013; 27: 301–6.

Brown RE, Basheer R, McKenna JT, Strecker RE, McCarley RW. Control of sleep and wakefulness. Physiol Rev 2012; 92: 1087–187.

Chatila M, Milleret C, Rougeul A, Buser P. Alpha rhythm in the cat thalamus. C R Acad Sci III 1993; 316: 51–8.

Clemens B, Bessenyei M, Piros P, Tóth M, Seress L, Kondákor I. Characteristic distribution of interictal brain electrical activity in idiopathic generalized epilepsy. Epilepsia 2007; 48: 941–9.

Clemens B. Valproate decreases EEG synchronization in a use-dependent manner in idiopathic generalized epilepsy. Seizure 2008; 17: 224–33.

Cox RW, Reynolds RC, Taylor PA. AFNI and clustering: false positive rates redux. BioRxiv 2016; 26: 1–15.

Damasio AR. On some functions of the human prefrontal cortex. Ann N Y Acad Sci 1995; 769: 241–51.

de Munck JC, Gonçalves SI, Huijboom L, Kuijer JP, Pouwels PJ, Heethaar RM, et al. The hemodynamic response of the alpha rhythm: an EEG/fMRI study. Neuroimage 2007; 35: 1142–51.

Difrancesco MW, Holland SK, Szaflarski JP. Simultaneous EEG/functional magnetic resonance imaging at 4 Tesla: correlates of brain activity to spontaneous alpha rhythm during relaxation. J Clin Neurophysiol 2008; 25: 255–64.

Elliott R, Dolan RJ, Frith CD. Dissociable functions in the medial and lateral orbitofrontal cortex: evidence from human neuroimaging studies. Cereb Cortex 2000; 10: 308–17.

Eklund A, Andersson M, Josephson C, Johannesson M, Knutsson H. Does parametric fMRI analysis with SPM yield valid results? An empirical study of 1484 rest datasets. Neuroimage 2012; 61: 565–78.

Eklund A, Nichols TE, Knutsson H. Cluster failure: why fMRI inferences for spatial extent have inflated false-positive rates. Proc Natl Acad Sci USA 2016; 113: 7900–5.

Feige B, Scheffler K, Esposito F, Di Salle F, Hennig J, Seifritz E. Cortical and subcortical correlates of electroencephalographic alpha rhythm modulation. J Neurophysiol 2005; 93: 2864–72.

Fink GR, Markowitsch HJ, Reinkemeier M, Bruckbauer T, Kessler J, Heiss WD. Cerebral representation of one's own past: neural networks involved in autobiographical memory. J Neurosci 1996; 16: 4275–82.

Friston KJ, Williams S, Howard R, Frackowiak RS, Turner R. Movement-related effects in fMRI time-series. Magn Reson Med 1996; 35: 346–55.

Fuentealba P, Steriade M. The reticular nucleus revisited: intrinsic and network properties of a thalamic pacemaker. Prog Neurobiol 2005; 75: 125–41.

Galizia EC, Myers CT, Leu C, de Kovel CG, Afrikanova T, Cordero-Maldonado ML, et al. CHD2 variants are a risk factor for photosensitivity in epilepsy. Brain 2015; 138: 1198–207.

Genovese CR, Lazar NA, Nichols T. Thresholding of statistical maps in functional neuroimaging using the false discovery rate. Neuroimage 2002; 15: 870–8.

Giannakodimos S, Panayiotopoulos CP. Eyelid myoclonia with absences in adults: a clinical and video-EEG study. Epilepsia 1996; 37: 36–44.

Goldman RI, Stern JM, Engel J Jr, Cohen MS. Simultaneous EEG and fMRI of the alpha rhythm. Neuroreport 2002; 13: 2487–92.

Gonçalves SI, de Munck JC, Pouwels PJ, Schoonhoven R, Kuijer JP, Maurits NM, et al. Correlating the alpha rhythm to BOLD using simultaneous EEG/fMRI: inter-subject variability. Neuroimage 2006; 30: 203–13.

Gregory RP, Oates T, Merry RT. Electroencephalogram epileptiform abnormalities in candidates for aircrew training. Electroencephalogr Clin Neurophysiol 1993; 86: 75–7.

Groppa S, Siebner HR, Kurth C, Stephani U, Siniatchkin M. Abnormal response of motor cortex to photic stimulation in idiopathic generalized epilepsy. Epilepsia 2008; 49: 2022–9.

Guerrini R, Dravet C, Genton P, Bureau M, Bonanni P, Ferrari AR, et al. Idiopathic photosensitive occipital lobe epilepsy. Epilepsia 1995; 36: 883–91.

Henssen A, Zilles K, Palomero-Gallagher N, Schleicher A, Mohlberg H, Gerboga F, et al. Cytoarchitecture and probability maps of the human medial orbitofrontal cortex. Cortex 2016; 75: 87–112.

Hughes SW, Crunelli V. Thalamic mechanisms of EEG alpha rhythms and their pathological implications. Neuroscientist 2005; 11: 357–72.

Kaas JH, Lyon DC. Pulvinar contributions to the dorsal and ventral streams of visual processing in primates. Brain Res Rev 2007; 55: 285–96.

Kasteleijn-Nolst Trenité DG, Binnie CD, Harding GF, Wilkins A. Photic stimulation: standardization of screening methods. Epilepsia 1999; 40: 75–9.

Kasteleijn-Nolst Trenité DG, Guerrini R, Binnie CD, Genton P. Visual sensitivity and epilepsy: a proposed terminology and classification for clinical and EEG phenomenology. Epilepsia 2001; 42: 692–701.

Klimesch W, Sauseng P, Hanslmayr S. EEG alpha oscillations: the inhibition-timing hypothesis. Brain Res Rev 2007; 53: 63–88.

Krauth A, Blanc R, Poveda A, Jeanmonod D, Morel A, Székely G. A mean three-dimensional atlas of the human thalamus: generation from multiple histological data. Neuroimage 2010; 49: 2053–62.

Jeavons PM. Nosological problems of myoclonic epilepsies in childhood and adolescence. Dev Med Child Neurol 1977; 19: 3–8.

Larsson PG, Kostov H. Lower frequency variability in the alpha activity in EEG among patients with epilepsy. Clin Neurophysiol 2005; 116: 2701–6.

Larsson PG, Eeg-Olofsson O, Lantz G. Alpha frequency estimation in patients with epilepsy. Clin EEG Neurosci 2012; 43: 97–104.

Laufs H, Kleinschmidt A, Beyerle A, Eger E, Salek-Haddadi A, Preibisch C, et al. EEG-correlated fMRI of human alpha activity. Neuroimage 2003; 19: 1463–76.

Laufs H, Lengler U, Hamandi K, Kleinschmidt A, Krakow K. Linking generalized spike-and-wave discharges and resting state brain activity by using EEG/fMRI in a patient with absence seizures. Epilepsia 2006; 47: 444–8.

Lindgren KA, Larson CL, Schaefer SM, Abercrombie HC, Ward RT, Oakes TR, et al. Thalamic metabolic rate predicts EEG alpha power in healthy control subjects but not in depressed patients. Biol Psychiatry 1999; 45: 943–52.

Liu Z, de Zwart JA, Yao B, van Gelderen P, Kuo LW, Duyn JH. Finding thalamic BOLD correlates to posterior alpha EEG. Neuroimage 2012; 63: 1060–9.

Lopes da Silva FH, van Lierop TH, Schrijer CF, van Leeuwen WS. Organization of thalamic and cortical alpha rhythms: spectra and coherences. Electroencephalogr Clin Neurophysiol 1973; 35: 627–39.

Lopes da Silva FH, Vos JE, Mooibroek J, Van Rotterdam A. Relative contributions of intracortical and thalamo-cortical processes in the generation of alpha rhythms, revealed by partial coherence analysis. Electroencephalogr Clin Neurophysiol 1980; 50: 449–56.

Lorincz ML, Kekesi KA, Juhasz G, Crunelli V, Hughes SW. Temporal framing of thalamic relay-mode firing by phasic inhibition during the alpha rhythm. Neuron 2009; 63: 683–96.

Makeig S, Debener S, Onton J, Delorme A. Mining event-related brain dynamics. Trends Cogn Sci 2004a; 8: 204–10.

Makeig S, Delorme A, Westerfield M, Jung TP, Townsend J, Courchesne E. Electroencephalographic brain dynamics following manually responded visual targets. PLoS Biol 2004b; 2: e176.

Mayhew SD, Ostwald D, Porcaro C, Bagshaw AP. Spontaneous EEG alpha oscillation interacts with positive and negative BOLD responses in the visual-auditory cortices and default-mode network. Neuroimage 2013; 76: 362–72.

Mazaheri A, Jensen O. Rhythmic pulsing: linking ongoing brain activity with evoked responses. Front Hum Neurosci 2010; 4: 177.

Miyauchi T, Endo K, Yamaguchi T, Hagimoto H. Computerized analysis of EEG background activity in epileptic patients. Epilepsia 1991; 32: 870–81.

Moeller F, Siebner HR, Ahlgrimm N, Wolff S, Muhle H, Granert O, et al. fMRI activation during spike and wave discharges evoked by photic stimulation. Neuroimage 2009; 48: 682–95.

Moeller F, Muthuraman M, Stephani U, Deuschl G, Raethjen J, Siniatchkin M. Representation and propagation of epileptic activity in absences and generalized photoparoxysmal responses. Hum Brain Mapp 2013; 34: 1896–909.

Morel A, Magnin M, Jeanmonod D. Multiarchitectonic and stereotactic atlas of the human thalamus. J Comp Neurol 1997; 387: 588–630.

Moosmann M, Ritter P, Krastel I, Brink A, Thees S, Blankenburg F, et al. Correlates of alpha rhythm in functional magnetic resonance imaging and near infrared spectroscopy. Neuroimage 2003; 20: 145–58.

Moruzzi G, Magoun HW. Brain stem reticular formation and activation of the EEG. Electroencephalogr Clin Neurophysiol 1949; 1: 455–73.

Nichols T, Hayasaka S. Controlling the familywise error rate in functional neuroimaging: a comparative review. Stat Methods Med Res 2003; 12: 419–46.

Nunez PL, Wingeier BM, Silberstein RB. Spatial-temporal structures of human alpha rhythms: theory, microcurrent sources, multiscale measurements, and global binding of local networks. Hum Brain Mapp 2001; 13: 125–64.

Omata K, Hanakawa T, Morimoto M, Honda M. Spontaneous slow fluctuation of EEG alpha rhythm reflects activity in deep-brain structures: a simultaneous EEG-fMRI study. PLoS One 2013; 8: e66869.

Pessoa L, Adolphs R. Emotion processing and the amygdala: from a 'low road' to 'many roads' of evaluating biological significance. Nat Rev Neurosci 2010; 11: 773–83.

Pyrzowski J, Siemiński M, Sarnowska A, Jedrzejczak J, Nyka WM. Interval analysis of interictal EEG: pathology of the alpha rhythm in focal epilepsy. Sci Rep 2015; 5: 16230.

Porciatti V, Bonanni P, Fiorentini A, Guerrini R. Lack of cortical contrast gain control in human photosensitive epilepsy. Nat Neurosci 2000; 3: 259–63.

Pfurtscheller G, Stancák A Jr, Neuper C. Post-movement beta synchronization. A correlate of an idling motor area? Electroencephalogr Clin Neurophysiol 1996; 98: 281–93.

Ritter P, Moosmann M, Villringer A. Rolandic alpha and beta EEG rhythms' strengths are inversely related to fMRI-BOLD signal in primary somatosensory and motor cortex. Hum Brain Mapp 2009; 30: 1168–87.

Ruggieri A, Vaudano AE, Benuzzi F, Serafini M, Gessaroli G, Farinelli V, et al. Mapping (and modeling) physiological movements during EEG-fMRI recordings: the added value of the video acquired simultaneously. J Neurosci Methods 2015; 239: 223–37.

Sadaghiani S, Scheeringa R, Lehongre K, Morillon B, Giraud AL, Kleinschmidt A. Intrinsic connectivity networks, alpha oscillations, and tonic alertness: a simultaneous electroencephalography/functional magnetic resonance imaging study. J Neurosci 2010; 30: 10243–50.

Scheeringa R, Fries P, Petersson KM, Oostenveld R, Grothe I, Norris DG et al. Neuronal Dynamics underlying high- and low-frequency EEG oscillations contribute independently to the human BOLD signal. Neuron 2011; 69: 572–3.

Scheeringa R, Petersson KM, Kleinschmidt A, Jensen O, Bastiaansen MC. EEG α power modulation of fMRI resting-state connectivity. Brain Connect 2012; 2: 254–64.

Siniatchkin M, Moeller F, Shepherd A, Siebner H, Stephani U. Altered cortical visual processing in individuals with a spreading photoparoxysmal EEG response. Eur J Neurosci 2007; 26: 529–36.

Striano S, Striano P, Nocerinoi C, et al. Eyelid myoclonia with absences: an overlooked epileptic syndrome?. Neurophysiol Clin 2002; 32: 287–96.

Strigaro G, Prandi P, Varrasi C, Monaco F, Cantello R. Defective visual inhibition in photosensitive idiopathic generalized epilepsy. Epilepsia 2012; 53: 695–704.

Strigaro G, Falletta L, Varrasi C, Rothwell JC, Cantello R. Overactive visuomotor connections underlie the photoparoxysmal response. A TMS study. Epilepsia 2015; 56: 1828–35.

Stoller A. Slowing of the alpha-rhythm of the electroencephalogram and its association with mental deterioration and epilepsy. J Ment Sci 1949; 95: 972–84.

Tyvaert L, Levan P, Grova C, Dubeau F, Gotman J. Effects of fluctuating physiological rhythms during prolonged EEG-fMRI studies. Clin Neurophysiol 2008; 119: 2762–74.

Toscani M, Marzi T, Righi S, Viggiano MP, Baldassi S. Alpha waves: a neural signature of visual suppression. Exp Brain Res 2010; 207: 213–19.

van Essen DC. A population-average, landmark- and surface-based (PALS) atlas of human cerebral cortex. Neuroimage 2005; 28: 635–62.

Varotto G, Visani E, Canafoglia L, Franceschetti S, Avanzini G, Panzica F. Enhanced frontocentral EEG connectivity in photosensitive generalized epilepsies: a partial directed coherence study. Epilepsia 2012; 53: 359–67.

Vaudano AE, Ruggieri A, Tondelli M, Avanzini P, Benuzzi F, Gessaroli G, et al. The visual system in eyelid myoclonia with absences. Ann Neurol 2014; 76: 412–27.

Visani E, Varotto G, Binelli S, Fratello L, Franceschetti S, Avanzini G, et al. Photosensitive epilepsy: spectral and coherence analyses of EEG using 14 Hz intermittent photic stimulation. Clin Neurophysiol 2010; 121: 318–24.

Volkmann FC. Human visual suppression. Vision Res 1986; 26: 1401–16.

Waltz S, Christen HJ, Doose H. The different patterns of the photoparoxysmal response–a genetic study. Electroencephalogr Clin Neurophysiol 1992; 83: 138–45.

Wilkins AJ, Bonanni P, Porciatti V, Guerrini R. Physiology of human photosensitivity. Epilepsia 2004; 45: 7–13.

Wolf P, Goosses R. Relation of photosensitivity to epileptic syndromes. J Neurol Neurosurg Psychiatry 1986; 49: 1386–91.

Wolf P, Yacubian EM, Avanzini G, Sander T, Schmitz B, Wandschneider B, et al. Juvenile myoclonic epilepsy: a system disorder of the brain. Epilepsy Res 2015; 114: 2–12.